· Article · Advances in Polar Science
doi: 10.13679/j.advps.2022.0095 September 2022 Vol. 33 No. 3: 235-243

Concentration maxima of methane in the bottom waters over the Chukchi Sea shelf: implication of its biogenic source

LI Yuhong[1], ZHANG Jiexia[1], YE Wangwang[1], JIN Haiyan[2], ZHUANG Yanpei[3] & ZHAN Liyang[1*]

[1] Key Laboratory of Global Change and Marine–Atmospheric Chemistry (GCMAC) of Ministry of Natural Resources (MNR), Third Institute of Oceanography (TIO), MNR, Xiamen 361005, China;
[2] Laboratory of Marine Ecosystem and Biogeochemistry, Second Institute of Oceanography, MNR, Hangzhou 310012, China;
[3] Polar and Marine Research Institute, Jimei University, Xiamen 361021, China

Received 1 July 2022; accepted 7 September 2022; published online 30 September 2022

Abstract Knowledge about the distribution of CH_4 remains insufficient due to the scarcity of data in the Arctic shelves. We conducted shipboard observations over the Chukchi Sea shelf (CSS) in the western Arctic Ocean in September 2012 to obtain the distribution and source characteristics of dissolved CH_4 in seawater. The oceanographic data indicated that a salinity gradient generated a pronounced pycnocline at depths of 20–30 m. The vertical diffusion of biogenic elements was restricted, and these elements were trapped in the bottom waters. Furthermore, high CH_4 concentrations were measured below the pycnocline, and low CH_4 concentrations were observed in the surface waters. The maximum concentrations of nutrients simultaneously occurred in the dense and cold bottom waters, and significant correlations were observed between CH_4 and SiO_3^{2-}, PO_4^{3-}, NO_2^-, and NH_4^+ ($p<0.01$, $n=44$). These results suggest that the production of CH_4 in the CSS has a similar trend as that of nutrient regeneration and is probably associated with the degradation of organic matter. The high primary productivity and high concentration of organic matter support the formation of biogenic CH_4 in the CSS and the subsequent release of CH_4 to the water column.

Keywords **Chukchi Sea shelf**, **methane**, **sources**, **nutrient**, **organic carbon**, **organic matter**

Citation: Li Y H, Zhang J X, Ye W W, et al. Concentration maxima of methane in the bottom waters over the Chukchi Sea shelf: implication of its biogenic source. Adv Polar Sci, 2022, 33(3): 235-243, doi: 10.13679/j.advps.2022.0095

1 Introduction

Methane (CH_4) is the most abundant hydrocarbon in the atmosphere and plays an important role in radiation balance and atmospheric chemistry (Cicerone and Oremland, 1988). The atmospheric CH_4 concentration has been increasing steadily, with a modern-day level of 1.91 ppmv (parts per million by volume), which is more than twice the preindustrial value of 0.71 ppmv (IPCC, 2007). CH_4 accounts for 15%–20% of the radiative forcing, and the elevated CH_4 concentration has further intensified greenhouse effects (Chappellaz et al., 1993). To understand the dynamics of atmospheric CH_4, various sources of natural CH_4 need to be constrained.

Oceans are net sources of atmospheric CH_4 (Bange et al., 1994; Bates et al., 1996), and 6–12 Tg CH_4 are emitted from the global ocean per year (Weber et al., 2019). Methanogenesis, an anaerobic microbial process

* Corresponding author, ORCID: 0000-0002-1380-453X, E-mail: zhanliyang@tio.org.cn

mediated by archaea, amounts to approximately 0.1% of ocean primary productivity, is most prevalent in sediments with a high sedimentation rate (Henrichs and Reeburgh, 1987; Reeburgh, 2007), and is thought to dominate marine CH_4 emissions. However, seepages of thermogenic CH_4 and the breakdown of CH_4 hydrates may also be significant contributors to these emissions (Kvenvolden and Rogers, 2005). Recent estimates suggest that 7×10^5–4×10^6 Tg CH_4 are stored as hydrates in the ocean (Buffett and Archer, 2004); this value is at least 2 orders of magnitude larger than the atmospheric CH_4 reservoir (~ 5000 Tg).

A large amount of organic carbon is buried in Arctic Ocean sediments (Gramberg et al., 1983; Shakhova and Semiletov, 2007), which makes the Arctic Ocean a potential CH_4 source. The Arctic Ocean is particularly sensitive to global warming, and the effects of warming on ecosystems will be the most dramatic in the Arctic (Holland and Bitz, 2003). Recently, many studies have proposed that the Arctic shelf is an important CH_4 source, and an additional release of CH_4 might result from the temperature destabilization of gas hydrates on the shallow continental shelves in the Laptev and East Siberian Seas (Shakhova and Semiletov, 2007; Shakhova et al., 2010), Spitsbergen continental margin (Damm et al., 2005; Westbrook et al., 2009). Organic matter stored in the sediment might be mobilized onto the shelves, leading to further biogenic CH_4 release via methanogenesis in the White Sea and Storfjorden (Savvichev et al., 2004; Damm et al., 2007). However, the sources of CH_4 are still not well understood in the Arctic shelf due to the complexity of the processes involved and the difficult access to these remote regions. In the Chukchi Sea, limited research has revealed CH_4 accumulation in the bottom waters (Li et al., 2017; Kudo et al., 2018; Bui et al., 2019). In conjunction with $\delta^{13}C_{CH4}$ values (Fenwick et al., 2017; Kudo et al., 2022), the most likely CH_4 source in this region is biogenic production, resulting from the decomposition of organic carbon in the seafloor. To date, it is believed that methane from the Arctic continental shelf is dominated by thermogenic origin, with a secondary of biogenic source (Berchet et al., 2020).

In this study, we present data for CH_4 in a water column over the Chukchi Sea shelf (CSS). We were able to obtain the characteristics of the vertical distribution of CH_4 in relation to the water mass structure. We also compare CH_4 with nutrient data and discuss possible processes that produce CH_4 in seawater.

2 Study area and methodology

2.1 Study area and its hydrographic setting

The CSS is one of the largest continental shelves in the world and has high biological productivity; Pacific Ocean waters transit through the Bering Strait and enter the Chukchi Sea (Figure 1). Three main transport pathways have been identified in the CSS: the inflow of warmer, fresher Alaskan Coastal Current (ACC) waters through the eastern channel (Coachman and Aagaard, 1966; Gong and Pickart, 2015); the transport of Bering Shelf Water (BSW) through the central channel between the Herald and Hanna Shoals (Woodgate et al., 2005); and the transport of colder, saltier, more nutrient-rich Anadyr Water in the west, which tends to follow Hope Valley toward Herald Canyon (Weingartner et al., 2005). Shipboard observations were conducted on the R/V *Xuelong* during the 5th Chinese National Arctic Research Expedition (CHINARE); seawater samples for CH_4 and other parameters were collected along 169°E meridian (named SR section) in September 2012. The sampling depths were 5, 20, 30, 40, 50, 70, 100 m and 5 m above sea floor.

2.2 Methods

CH_4 samples were transferred to a Biochemical Oxygen Demand (BOD) bottle (250 mL), with approximately twofold overflow of the bottle volume to avoid bubbles. To inhibit biological activity, 120 μL of saturated $HgCl_2$ solution was added to the water samples. The bottles were sealed with greased stoppers that were then fixed with a clip. The sample bottles were kept in the dark at 4 ℃ until transport back to the laboratory on land for analysis. Subsamples were taken following the method of Butler and Elkins (1991). The headspace method was adopted to pretreat the water samples, and high-purity N_2 was introduced to create an around 7 mL headspace in 50 mL preweighed bottles. After shaking for 1 h at 30.0 ℃, full equilibrium was achieved. The 5-mL gas samples were injected into an Agilent 7890A gas chromatography equipped with a flame ionization detector (FID). The CH_4 gas standards were provided by the National Institute of Metrology, China. There is a linear relationship between the FID signal and the CH_4 concentration; a single-point standard was inserted after every 12 samples to enable assessment of the drift of the FID. The precision of repeated analyses of 10 water samples was approximately 5% (Li et al., 2017).

The *in situ* CH_4 equilibrium concentration was calculated from solubility measurements based on the method proposed by Wiesenburg and Guinasso (1979). Nutrient samples (nitrate, silicate, phosphate, nitrite, and ammonium) for seawater were filtered through prewashed cellulose acetate membranes (0.45 μm) and measured immediately using a continuous flow analyzer Skarlar San++ (Holland, Breda). The detection limits were 0.1 $\mu mol \cdot L^{-1}$ for NO_3^-, 0.1 $\mu mol \cdot L^{-1}$ for SiO_3^{2-}, 0.03 $\mu mol \cdot L^{-1}$ for PO_4^{3-}, 0.01 $\mu mol \cdot L^{-1}$ for NO_2^-, and 0.02 $\mu mol \cdot L^{-1}$ for NH_4^+. Seawater salinity and temperature data were processed by using the standard SBE CTD procedure and obtained from the National Arctic and Antarctic Data Center (http://www.chinare.org.cn).

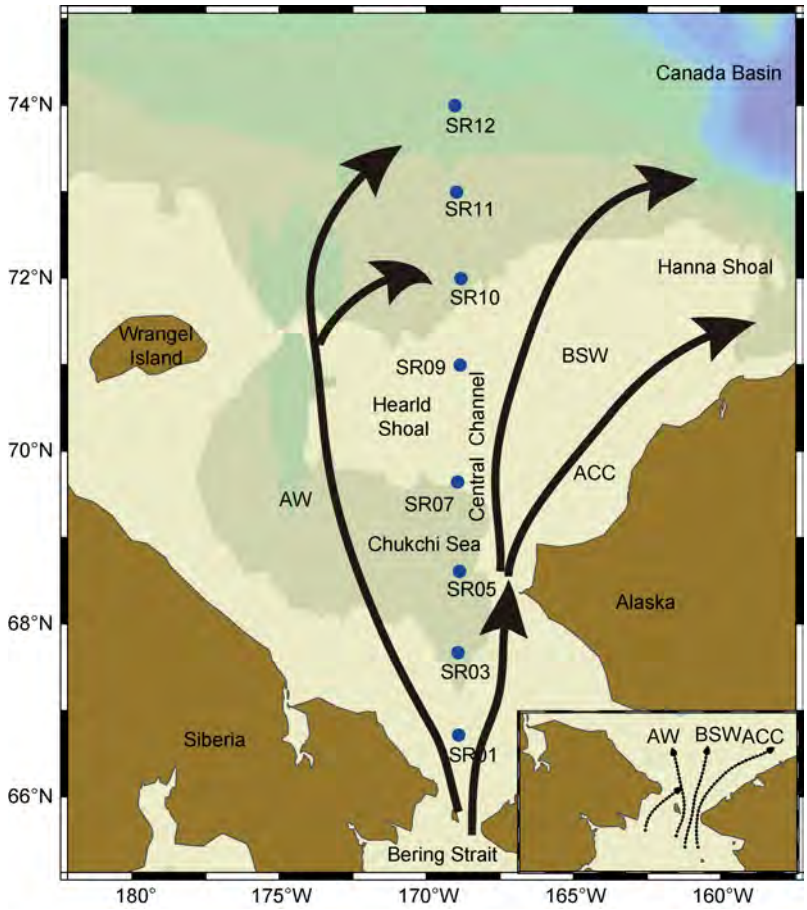

Figure 1 Sampling stations along the SR section (blue circles) in the CSS during the 5th CHINARE. The inflow of the Bering Strait is separated into three main branches: Anadyr Water (AW), Bering Shelf Water (BSW), and Alaska Coastal Water (ACC).

3 Results and discussion

3.1 Hydrology and nutrient distributions

Due to the influence of warm and saline Pacific water and cold and fresh ice-melt water, wide temperature and salinity ranges were observed in the water column of the SR transect, with values ranging from approximately −1.6–7.6℃ and 26.4–34.4, respectively (Figure 2). Cold and even freezing temperatures were observed in the northern bottom region, and warm water was distributed mainly in the southern surface layer. High-salinity (>32) water was present only in the bottom of the column, whereas low-salinity water (<32) water was widely distributed in the narrow surface waters. The distribution pattern of temperature was the opposite of that of salinity along the transect. Despite the change in temperature, the pattern of potential density was similar to that of salinity, which indicates that the water masses were mainly controlled by salinity. High stratifications could be observed in the distribution patterns, with the intensive dispersal of dense water masses at the bottom and vice versa.

Physical characteristics of the water masses were identified (Figure 3), and high-temperature and low-salinity waters (T≈6℃, S≈27) on the southern surface were distinguished from BSW (Walsh et al., 1989). An extremely fresh and relatively cold water mass (T≈−1℃, S≈27) in the northern surface typically originates from near-surface ice-melt water (SIMW) (Weingartner et al., 2005). A high-salinity water with freezing temperatures (T≈0℃, S≈33) dispersed in the bottom layer is typically regarded as a portion of remnant winter-transformed water (WW) from the previous winter (Weingartner et al., 1998; Spall, 2007). In the study area, a salinity gradient generated a pronounced pycnocline at depths of 20–30 m, and vertical diffusive transport and the mixing of biogenic elements were restricted and trapped in the bottom waters.

The distribution of nutrients ($NO_3^- + NO_2^-$) over the CSS is presented in Figure 2, and all nutrients showed a similar distribution pattern (not shown), and concentrations increased with depth. The concentrations were as high as > 20 μmol·L^{-1} (NO_3^-), >30 μmol·L^{-1} (SiO_3^{2-}), >2 μmol·L^{-1} (PO_4^{3-}), >4 μmol·L^{-1} (NH_4^+) and >0.2 μmol·L^{-1} (NO_2^-) in the same water mass, indicating possible efflux from the sediment. High values were located in the bottom waters of

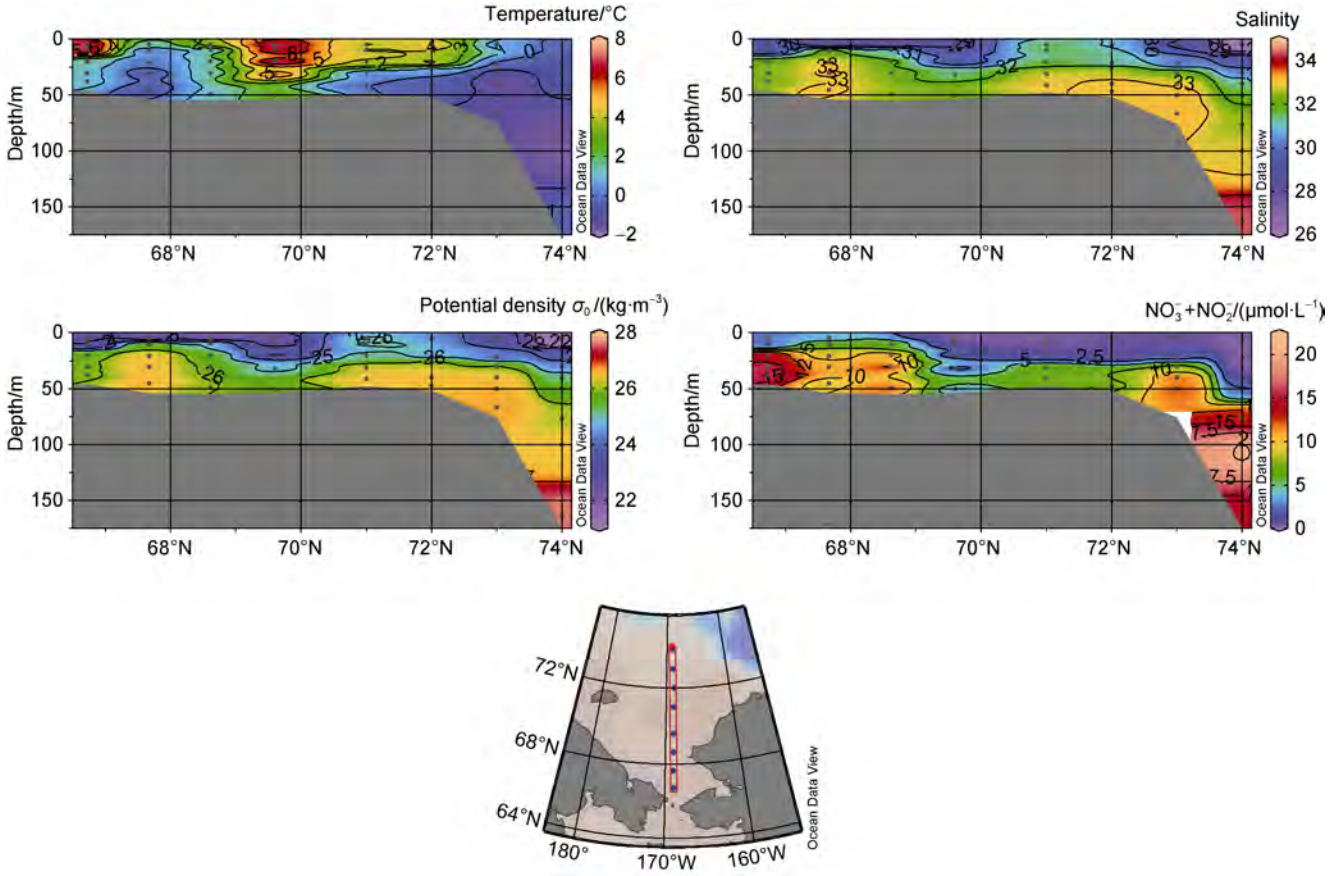

Figure 2 Distributions of temperature, salinity, potential density and nutrients (NO_3^- + NO_2^-) in the SR section of the CSS.

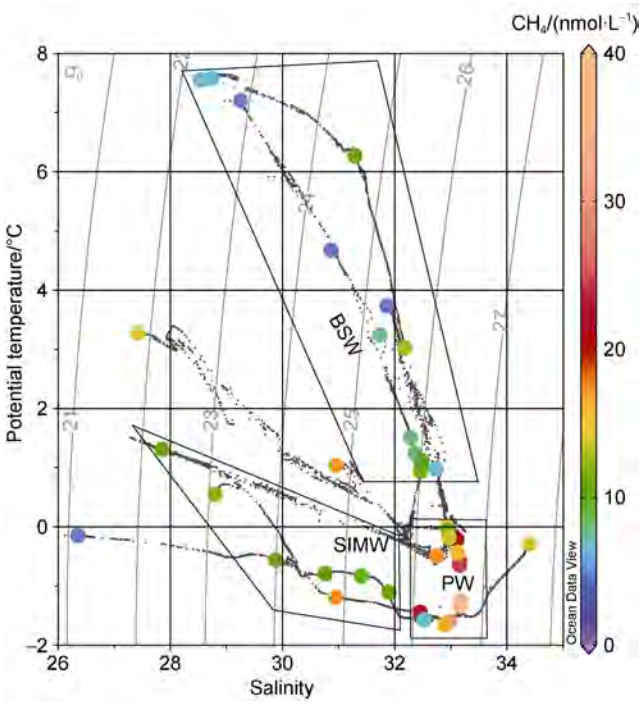

Figure 3 Temperature-salinity diagrams and CH_4 concentrations in the SR section of the CSS.

SR03, SR05, and SR11, where a "biological hotspot" is known to exist (Grebmeier et al., 2015). In the northern surface waters, nutrient concentrations were very low (SiO_3^{2-} : ~5 μmol·L^{-1}, PO_4^{3-} : ~0.5 μmol·L^{-1}) and even under the detection limit (NO_3^- , NH_4^+ and NO_2^-). Table 1 shows the concentrations of nutrients in different water masses, with the highest concentrations of nutrients in the WW and the lowest concentration of nutrients in the SIMW, corresponding to the dense bottom waters and the north surface waters of the CSS, respectively. The high concentrations of nutrients in the WW are attributed to the regeneration of organic matter that has settled down to the sediment. In contrast, the low concentrations of nutrients in the northern surface layer (SIMW) can be explained by biological consumption, and the strong stratification limits the vertical mixing of bottom waters rich in nutrients to the surface.

3.2 Distributions of CH_4 in the CSS

The vertical distribution of CH_4 along section SR is presented in Figure 4, showing that the CH_4 concentrations showed marked variations; CH_4 in the surface waters (approximately 5 m below the sea surface) ranged from 4.6 nmol·L^{-1} to 14.6 nmol·L^{-1}, which were significantly

Table 1 Mean (in brackets) and variation ranges of the main parameters in different water masses in the CSS

Parameter	Water masses		
	BSW	SIMW	WW
Temperature/℃	1.4–7.6 (5.4)	−1.4–0.65 (−0.2)	−1.6–1.6 (−0.2)
Salinity	27.4–31.9 (29.7)	26.4–30.5 (29.0)	31.4–34.4 (32.8)
CH_4/(nmol·L^{-1})	4.6–14.6 (7.3)	4.7–17.5 (10.9)	6.7–38.8 (16.7)
DO/(mg·L^{-1})	9.1–12.1 (10.0)	11.5–13.9 (12.6)	7.2–12.4 (9.6)
SiO_3^{2-} /(μmol·L^{-1})	2.1–15.9 (9.1)	2.7–14.9 (6.3)	5.0–50.8 (25.4)
NO_3^- /(μmol·L^{-1})	0.1–3.4 (1.1)	0.2–1.5 (0.6)	0.7–20.3 (10.4)
NH_4^+ /(μmol·L^{-1})	0.1–2.1 (0.9)	0.2–0.5 (0.3)	0.3–8.3 (3.6)
NO_2^- /(μmol·L^{-1})	0.02–0.13 (0.06)	0.01–0.05 (0.03)	0.05–0.40 (0.17)
PO_4^{3-} /(μmol·L^{-1})	0.6–0.9 (0.7)	0.5–0.8 (0.7)	1.0–2.3 (1.8)

higher values than the expected atmospheric equilibrium concentrations of 3.2–4.1 nmol·L^{-1}, with saturations from 114% to 398%. This result means that surface waters in the CSS were supersaturated with CH_4 and could be a potential source of atmospheric CH_4. In the water column, CH_4 concentrations ranged from 4.8 nmol·L^{-1} to 38.8 nmol·L^{-1}, and the maximum concentrations of CH_4 were distributed in the bottom waters of stations SR03, SR10, and SR11, representing CH_4 supersaturation of up to 962% in the dense and cold bottom waters of the CSS. The ambient dissolved oxygen (DO) of the water column ranged from 7.3 mg·L^{-1} to 13.9 mg·L^{-1}, with high concentrations located in the surface waters of stations SR03, SR11, SR12 and the lowest values at the bottom waters of the same stations. There were consistently high concentrations of CH_4 and low DO levels in the bottom waters of stations SR03, SR10 and SR11 (Figure 4, Table 1). Nutrient-rich Pacific water and sea-ice melting increase the light-stimulated primary production of ice algae and phytoplankton, maintaining high concentrations of DO in the surface and shallow depths, as well as low grazing pressure and a high flux of organic carbon settling to the seafloor (Grebmeier et al., 2006); furthermore, respiratory action consumes O_2 and reduces the concentration of DO in the bottom waters. In general, the distribution pattern of CH_4 is similar to that of salinity and potential density, with an increasing trend from the surface to bottom water (WW). Water masses are a factor controlling the gradient shape in the Chukchi Sea, suggesting that high concentrations of CH_4 are trapped below the pycnocline (Fenwick et al., 2017; Kudo et al., 2022); thus, the CH_4 concentration in surface waters is limited during the autumn stratification period (Kudo et al., 2022). The distribution of CH_4 showed a clear increasing downward gradient, indicating that high concentrations of CH_4 in near-bottom waters at these stations might correlate with the production and emission of CH_4 from the organic-rich sediment interface.

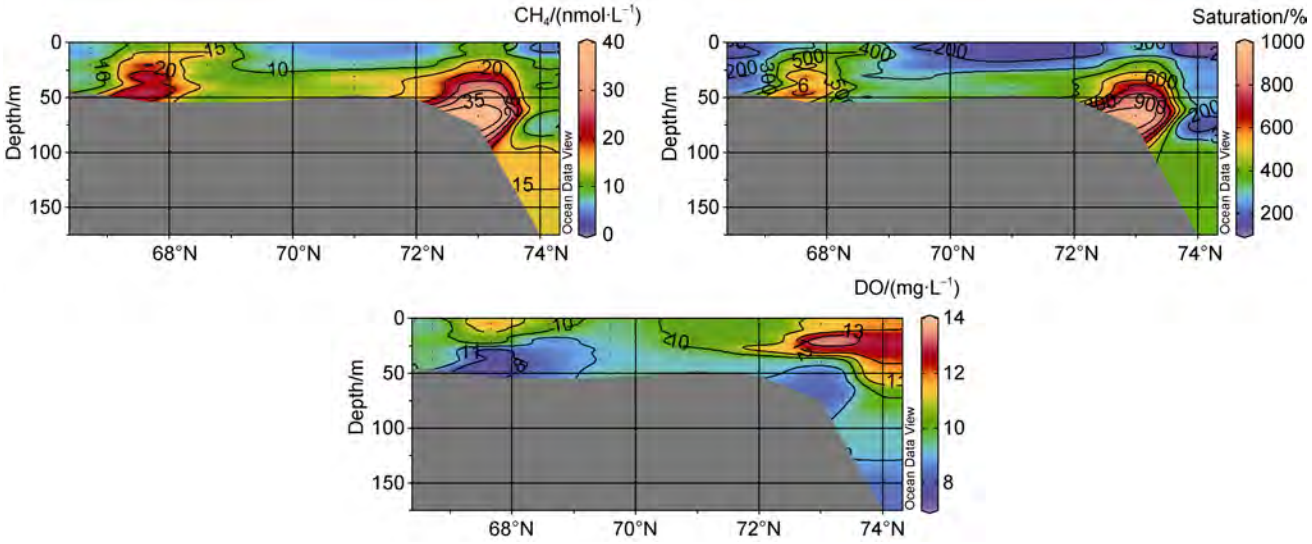

Figure 4 Distributions of methane (CH_4), methane saturations and dissolved oxygen (DO) in the SR section of the CSS.

3.3 Sources of CH_4 in the CSS

A correlation analysis was performed to identify the potential relationship between excess CH_4 (ΔCH_4) and nutrients (PO_4^{3-}, NH_4^+, NO_2^-, SiO_3^{2-}, and NO_3^-) for all the samples in the water column in the SR section, and scatter diagrams are shown in Figure 5. High-confidence coefficients were found between ΔCH_4 and PO_4^{3-} (r^2=0.46, p<0.01), NH_4^+ (r^2=0.46, p<0.01), NO_2^- (r^2=0.41, p<0.01), NO_3^- (r^2=0.16, p<0.01) and SiO_3^{2-} (r^2=0.34, p<0.01), and the high and low concentrations of CH_4 in different water masses corresponded well to the distribution of these nutrients. Less significant correlations were found between CH_4 and NO_3^-, which may be consumed through the significant denitrification process in the CSS (Devol et al., 1997). We propose that CH_4 maxima in the bottom waters are produced through the microbial degradation of organic materials in the sediments, followed by the release of microbial generated CH_4 into the overlying waters. The Chukchi Sea is one of the most productive areas in the Arctic Ocean (Grebmeier et al., 2006), and high particulate organic carbon (POC) fluxes are exported down to the underlying sediments (Moran et al., 2005; Lepore et al., 2007). The organic carbon concentrations (0.65%–2.03%) in the sediments are higher than the average value of 0.75% for the world shelf (Berner, 1982), and the organic matter supports high concentrations of biogenic elements and high rates of methanogenesis processes in the upper sediment layers (Savvichev et al., 2007). In the northern Chukchi Sea, microbial methanogenesis in the sediments could also be found, which is attributed to primary production enhancing the organic-rich material flux to the seafloor (Lapham et al., 2017). In this study, due to high oxygen contents (7.24–12.38 $mg \cdot L^{-1}$) in the WW, the conditions were unfavorable for the production of CH_4; therefore, methanogenesis was evidently restricted to shelf sediments (Ivanov et al., 2002). Matveeva et al. (2015) presents the carbon stable isotopic composition of CH_4 samples (varying from −96.7‰ to −92.8.7‰), unambiguously demonstrating the microbial origin of CH_4. In the bottom layers of the CSS, the maximum CH_4 concentration was accompanied by lower $\delta^{13}C_{CH4}$ values, indicating that CH_4 was produced mainly by organic matter degradation via methanogens (Kudo et al., 2022). In addition, data obtained from the same water samples produced a positive relationship between ΔCH_4 and biogenic gas N_2O concentrations (unpublished data), with r^2=0.49 and p<0.01 (Table 2), and showed a coincident distribution pattern in the CSS, indicating that biological processes were responsible for the production of both gases. The high biological activity in the Chukchi Sea is called a biological hotspot (Nishino et al., 2016), and the significant amount of fresh organic matter in the sediment supports high rates of microbial processes. It is reasonable to deduce that the maximal CH_4 concentration in the bottom waters is related to sediment release in the CSS (Kudo et al., 2018, 2022).

3.4 Comparison with other areas in the Arctic Ocean

CH_4 can be produced through the bacterial degradation of organic materials in sediments and subsequent release into

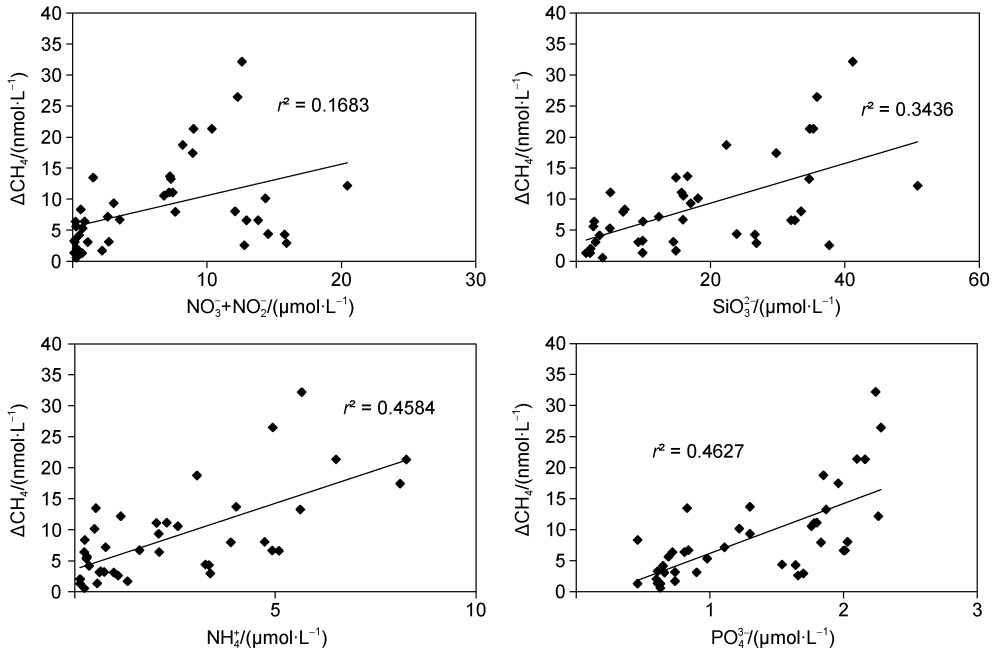

Figure 5 Correlation analysis between ΔCH_4 and $NO_3^- + NO_2^-$, SiO_3^{2-}, NH_4^+ and PO_4^{3-} in the water column of the SR section in the CSS.

Table 2 Correlation analysis between ΔCH_4 and $NO_3^- + NO_2^-$, NO_3^-, NO_2^-, SiO_3^{2-}, NH_4^+ and PO_4^{3-} with Pearson and Spearman models

	ΔCH_4 (nmol·L^{-1}) Pearson	ΔCH_4 (nmol·L^{-1}) Spearman
N_2O/(nmol·L^{-1})	0.70**	0.81**
$NO_3^- + NO_2^-$ /(μmol·L^{-1})	0.41**	0.50**
NO_3^- /(μmol·L^{-1})	0.40**	0.50**
NO_2^- /(μmol·L^{-1})	0.64**	0.57**
SiO_3^{2-} /(μmol·L^{-1})	0.59**	0.59**
NH_4^+ /(μmol·L^{-1})	0.68**	0.63**
PO_4^{3-} /(μmol·L^{-1})	0.68**	0.73**

Note: ** p<0.01, indicating all correlations are significant at the 0.01 level.

the overlying near-bottom waters through sediment water exchange, seepages of thermogenic methane from the decomposition of hydrates, the leakage of gas, and serpentinization reactions that may occur in specific areas (Reeburgh, 2007). As this area does not apparently contain subsea permafrost or gas hydrates (Ruppel, 2015), and $\delta^{13}C_{CH4}$ values are indicative of biogenic production (Whiticar and Faber, 1986), the most likely CH_4 source in this region is seafloor methanogenesis resulting from the decomposition of organic carbon (Fenwick et al., 2017). In the CSS areas, the concentrations in the bottom layer were higher (up to 55.9 nmol·L^{-1}), whereas $\delta^{13}C$ values were lower (down to −63.8‰) than in the surface layer, indicating that CH_4 was produced mainly by organic matter degradation in seafloor sediment via methanogens (Kudo et al., 2022). As a result, the release of CH_4 from the sediments into the water column results in a dome-like structure of relatively high CH_4 concentrations in the dense bottom water of the CSS. We summarized CH_4 concentrations and sources in different areas of the Arctic Ocean (Table 3) and distinguished the origin of CH_4 from sedimentary release. Compared to the open ocean, in the East Siberia Sea, because of a lack of sunlight and highly turbid waters, primary production is suppressed by factors of 100 to 1000, whereas the CH_4 levels are elevated 10-fold, which could be attributed to the thawing of the subsea permafrost and the consequentially increased permeability for CH_4 (Shakhova et al., 2010). In SW-Spitsbergen, CH_4 concentrations 2 orders of magnitude higher than the equilibrium concentrations with the atmosphere are discharged from thermogenic processes or hydrate on top of sandy and gravelly banks, with distinctly heavy $\delta^{13}C_{CH4}$ values (Damm et al., 2005). The highest concentration of CH_4 in the White Sea and Storfjorden was approximately 50 nmol·L^{-1} in the bottom waters because of high accumulation rates of organic carbon (Damm et al., 2007; Savvichev et al., 2004); thus, both areas are ideal environments for the formation of biogenic methane near the sediment surface (Daniel and Jochen, 2005). For dome-like structure formation and turbulent mixing models, a dilution factor of 10^4 is assumed (Lupton et al., 1985). Therefore, a potential initial CH_4 concentration of approximately 0.4 mmol·L^{-1} in the sediments is sufficient to create a plume with the CH_4 concentrations detected in the CSS bottom waters (approximately 40 nmol·L^{-1}) and the maximum CH_4 concentration of 2 mmol·L^{-1} in the seafloor over the CSS (Matveeva et al., 2015). Indeed, the Chukchi Sea bottom sediments have been shown to support methanogenesis rates of up to 67 μmol·m^{-2}·d^{-1} (Savvichev et al., 2007). This intensive CH_4 production in shallow sediment could supply CH_4 to the bottom waters, resulting in high CH_4 concentrations (Fenwick et al., 2017). Thus, we suggest that the decomposition of organic carbon from primary production underlies the biogenic formation of CH_4 in the CSS.

Table 3 CH_4 concentrations and sources in different areas of the Arctic Ocean

Area	Date	Concentrations/(nmol·L^{-1})	Sources	References
Barents Sea	Aug. 1991	3.6–56.7	Not defined	Lammers et al., 1995
Beaufort Sea shelf	Apr.–May, 1992	10.7–111.8	Not defined	Kvenvolden et al., 1993
White Sea	1999–2001	3.56–53.57	Biogenic	Savvichev et al., 2004
Storfjorden	Mar. 2003	3.5–48.3	Biogenic	Damm et al., 2007
Spitsbergen	Summer of 2001	-	Thermogenic	Knies et al., 2004
SW-Spitsbergen	Jul. 2000 Sep. 2001	2–240	Thermogenic	Damm et al., 2005
East Siberia Sea	Sep., 2003–2008	22.6–246.2	Thermogenic	Shakhova et al., 2010
West Spitsbergen continental margin	Aug. 2010	10–524	Mixture of biogenic and thermogenic	Gentz et al., 2014
Laptev Sea	Jul. 2014	3–1511	Thermogenic	Steinbach et al., 2021
Chukchi Sea	Aug. 2004	8–31	Biogenic	Savvichev et al., 2007; Matveeva et al., 2015
	Sep. 2012	4.1–55.9	Biogenic	Kudo et al., 2018
	Sep. 2012	4.59–38.78	Biogenic	This study

4 Conclusion

Shipboard observations were conducted over the CSS in the western Arctic Ocean in September 2012 by the R/V *Xuelong* during the 5th CHINARE. Low concentrations of CH_4 (~ 10 nmol·L^{-1}) were observed in the surface BSW and SIMW, while high CH_4 concentrations were measured in the cold and dense WW, the layer in which the maximum concentrations of nutrients (NO_3^-, NH_4^+, SiO_3^{2-}, PO_4^{3-} and NO_2^-) occurred simultaneously. High correlations were found between CH_4 and PO_4^{3-} (r^2=0.46), NH_4^+ (r^2=0.46), NO_2^- (r^2=0.41), NO_3^- (r^2=0.16) and SiO_3^{2-} (r^2=0.34). These significant correlations imply similar mechanisms of production for both CH_4 and nutrients. The production of CH_4 is proposed to be relevant to the decomposition of organic matter in sediments. Compared with the thermogenic CH_4 from hydrate or fossil seepages in other Arctic shelf regions, the CSS is productive and demonstrates extremely high accumulation rates of organic carbon, which favors the formation of biogenic CH_4 in the sediment.

Acknowledgments This work was supported by the Scientific Research Foundation of the Third Institute of Oceanography, MNR (Grant nos. 2022011, 2018031 and 2018024) and the Natural Science Foundation of Fujian Province, China (Grant no. 2020J01102). We appreciate two anonymous reviewers, and Associate Editor Dr. Daiki Nomura for their constructive comments that have further improved the manuscript.

References

Bange H W, Bartell U H, Rapsomanikis S, et al. 1994. Methane in the Baltic and North Seas and a reassessment of the marine emissions of methane. Global Biogeochem Cycles, 8(4): 465-480, doi:10.1029/94gb02181.

Bates T S, Kelly K C, Johnson J E, et al. 1996. A reevaluation of the open ocean source of methane to the atmosphere. J Geophys Res, 101(D3): 6953-6961, doi:10.1029/95jd03348.

Berchet A, Pison I, Crill P M, et al. 2020. Using ship-borne observations of methane isotopic ratio in the Arctic Ocean to understand methane sources in the Arctic. Atmos Chem Phys, 20(6): 3987-3998, doi:10.5194/acp-20-3987-2020.

Berner R A. 1982. Burial of organic carbon and pyrite sulfur in the modern ocean: its geochemical and environmental significance. Am J Sci, 282(4): 451-473, doi:10.2475/ajs.282.4.451.

Buffett B, Archer D. 2004. Global inventory of methane clathrate: sensitivity to changes in the deep ocean. Earth Planet Sci Lett, 227(3-4): 185-199, doi:10.1016/j.epsl.2004.09.005.

Bui O T N, Kameyama S, Kawaguchi Y, et al. 2019. Influence of warm-core eddy on dissolved methane distributions in the southwestern Canada Basin during late summer/early fall 2015. Polar Sci, 22: 100481, doi:10.1016/j.polar.2019.100481.

Butler J H, Elkins J W. 1991. An automated technique for the measurement of dissolved N_2O in natural waters. Mar Chem, 34(1-2): 47-61, doi:10.1016/0304-4203(91)90013-M.

Chappellaz J, Bluniert T, Raynaud D, et al. 1993. Synchronous changes in atmospheric CH_4 and Greenland climate between 40 and 8 kyr BP. Nature, 366(6454): 443-445, doi:10.1038/366443a0.

Cicerone R J, Oremland R S. 1988. Biogeochemical aspects of atmospheric methane. Global Biogeochem Cycles, 2(4): 299-327, doi:10.1029/gb002i004p00299.

Coachman L K, Aagaard K. 1966. On the water exchange through Bering Strait. Limnol Oceanogr, 11(1): 44-59, doi:10.4319/lo.1966.11.1.0044.

Damm E, Mackensen A, Budéus G, et al. 2005. Pathways of methane in seawater: plume spreading in an Arctic shelf environment (SW-Spitsbergen). Cont Shelf Res, 25(12-13): 1453-1472, doi:10.1016/j.csr.2005.03.003.

Damm E, Schauer U, Rudels B, et al. 2007. Excess of bottom-released methane in an Arctic shelf sea polynya in winter. Cont Shelf Res, 27(12): 1692-1701, doi:10.1016/j.csr.2007.02.003.

Daniel W, Jochen K. 2005. Recent distribution and accumulation of organic carbon on the continental margin west of Spitsbergen, Geochem Geophy Geosy, 6(9): 117-134, doi:10.1029/2005GC000916.

Devol A H, Codispoti L A, Christensen J P. 1997. Summer and winter denitrification rates in western Arctic shelf sediments. Cont Shelf Res, 17(9): 1029-1050, doi:10.1016/S0278-4343(97)00003-4.

Fenwick L, Capelle D, Damm E, et al. 2017. Methane and nitrous oxide distributions across the North American Arctic Ocean during summer, 2015. J Geophys Res, 122(1): 390-412, doi:10.1002/2016JC012493.

Gentz T, Damm E, Schneider von Deimling J, et al. 2014. A water column study of methane around gas flares located at the West Spitsbergen continental margin. Cont Shelf Res, 72: 107-118, doi:10.1016/j.csr.2013.07.013.

Gong D, Pickart R S. 2015. Summertime circulation in the eastern Chukchi Sea. Deep Sea Res Part II Top Stud Oceanogr, 118: 18-31, doi:10.1016/j.dsr2.2015.02.006.

Gramberg I S, Kulakov Y N, Pogrebitskiy Y Y, et al. 1983. Arctic oil- and gas-bearing superbasin. Paper presented at the 11th World Petroleum Congress, London, UK, August 1983.

Grebmeier J M, Bluhm B A, Cooper L W, et al. 2015. Ecosystem characteristics and processes facilitating persistent macrobenthic biomass hotspots and associated benthivory in the Pacific Arctic. Prog Oceanogr, 136: 92-114, doi:10.1016/j.pocean.2015.05.006.

Grebmeier J M, Cooper L W, Feder H M, et al. 2006. Ecosystem dynamics of the Pacific-influenced northern Bering and Chukchi Seas in the Amerasian Arctic. Prog Oceanogr, 71(2-4): 331-361, doi:10.1016/j.pocean.2006.10.001.

Henrichs S M, Reeburgh W S. 1987. Anaerobic mineralization of marine sediment organic matter: rates and the role of anaerobic processes in the oceanic carbon economy. Geomicrobiol J, 5(3-4): 191-237, doi:10.1080/01490458709385971.

Holland M M, Bitz C M. 2003. Polar amplification of climate change in coupled models. Clim Dyn, 21(3): 221-232, doi:10.1007/s00382-003-0332-6.

Intergovernmental Panel on Climate Change (IPCC). 2007. Climate change 2007–the physical science basis: Working Group I contribution to the fourth assessment report of the IPCC. Cambridge: Cambridge University Press.

Ivanov M V, Pimenov N V, Rusanov I I, et al. 2002. Microbial processes of the methane cycle at the north-western shelf of the black sea. Estuar Coast Shelf Sci, 54(3): 589-599, doi:10.1006/ecss.2000.0667.

Knies J, Damm E, Gutt J, et al. 2004. Near-surface hydrocarbon anomalies in shelf sediments off Spitsbergen: evidences for past seepages. Geochem Geophys Geosyst, 5(6): 135112194, doi:10.1029/2003gc 000687.

Kudo K, Toyoda S, Yamada K, et al. 2022. Source analysis of dissolved methane in Chukchi Sea and Bering Strait during summer–autumn of 2012 and 2013. Mar Chem, 243: 104119, doi:10.1016/j.marchem. 2022.104119.

Kudo K, Yamada K, Toyoda S, et al. 2018. Spatial distribution of dissolved methane and its source in the western Arctic Ocean. J Oceanogr, 74(3): 305-317, doi:10.1007/s10872-017-0460-y.

Kvenvolden K A, Lilley M D, Lorenson T D, et al. 1993. The Beaufort Sea continental shelf as a seasonal source of atmospheric methane. Geophys Res Lett, 20(22): 2459-2462, doi:10.1029/93gl02727.

Kvenvolden K A, Rogers B W. 2005. Gaia's breath—global methane exhalations. Mar Petroleum Geol, 22(4): 579-590, doi:10.1016/j. marpetgeo.2004.08.004.

Lammers S, Suess E, Hovland M. 1995. A large methane plume east of Bear Island (Barents Sea): implications for the marine methane cycle. Geol Rundsch, 84(1): 59-66, doi:10.1007/BF00192242.

Lapham L, Marshall K, Magen C, et al. 2017. Dissolved methane concentrations in the water column and surface sediments of Hanna Shoal and Barrow Canyon, Northern Chukchi Sea. Deep Sea Res Part II Top Stud Oceanogr, 144: 92-103, doi:10.1016/j.dsr2.2017.01.004.

Lepore K, Moran S B, Grebmeier J M, et al. 2007. Seasonal and interannual changes in particulate organic carbon export and deposition in the Chukchi Sea. J Geophys Res, 112(C10): C10024, doi:10.1029/2006jc003555.

Li Y, Zhan L, Zhang J, et al. 2017. A significant methane source over the Chukchi Sea shelf and its sources. Cont Shelf Res, 148: 150-158, doi:10.1016/j.csr.2017.08.019.

Lupton J E, Delaney J R, Johnson H P, et al. 1985. Entrainment and vertical transport of deep-ocean water by buoyant hydrothermal plumes. Nature, 316(6029): 621-623, doi:10.1038/316621a0.

Matveeva T, Savvichev A, Semenova A, et al. 2015. Source, origin, and spatial distribution of shallow sediment methane in the Chukchi Sea. Oceanography, 28(3): 202-217, doi:10.5670/oceanog.2015.66.

Moran S B, Kelly R P, Hagstrom K, et al. 2005. Seasonal changes in POC export flux in the Chukchi Sea and implications for water column-benthic coupling in Arctic shelves. Deep Sea Res Part II Top Stud Oceanogr, 52(24-26): 3427-3451, doi:10.1016/j.dsr2.2005. 09.011.

Nishino S, Kikuchi T, Fujiwara A, et al. 2016. Water mass characteristics and their temporal changes in a biological hotspot in the southern Chukchi Sea. Biogeosciences, 13(8): 2563-2578, doi:10.5194/bg-13-2563-2016.

Reeburgh W S. 2007. Oceanic methane biogeochemistry. Chem Rev, 107(2): 486-513, doi:10.1021/cr050362v.

Ruppel C. 2015. Permafrost-associated gas hydrate: Is it really approximately 1% of the global system? J Chem Eng Data, 60(2): 429-436, doi:10.1021/je500770m.

Savvichev A S, Rusanov I I, Iusupov S K, et al. 2004. The biogeochemical cycle of methane in the coastal zone and littoral of the Kandalaksha Bay of the White Sea. Mikrobiologiia, 73(4): 540-552.

Savvichev A S, Rusanov I I, Pimenov N V, et al. 2007. Microbial processes of the carbon and sulfur cycles in the Chukchi Sea. Microbiology, 76(5): 603-613, doi:10.1134/s0026261707050141.

Shakhova N, Semiletov I. 2007. Methane release and coastal environment in the East Siberian Arctic shelf. J Mar Syst, 66(1-4): 227-243, doi:10.1016/j.jmarsys.2006.06.006.

Shakhova N, Semiletov I, Salyuk A, et al. 2010. Extensive methane venting to the atmosphere from sediments of the East Siberian Arctic Shelf. Science, 327(5970): 1246-1250, doi:10.1126/science.1182221.

Spall M A. 2007. Circulation and water mass transformation in a model of the Chukchi Sea. J Geophys Res, 112(C5): C05025, doi:10.1029/ 2005jc003364.

Steinbach J, Holmstrand H, Shcherbakova K, et al. 2021. Source apportionment of methane escaping the subsea permafrost system in the outer Eurasian Arctic Shelf. Proc Natl Acad Sci, 118(10): e2019672118, doi:10.1073/pnas.2019672118.

Walsh J J, McRoy C P, Coachman L K, et al. 1989. Carbon and nitrogen cycling within the Bering/Chukchi Seas: source regions for organic matter effecting AOU demands of the Arctic Ocean. Prog Oceanogr, 22(4): 277-359, doi:10.1016/0079-6611(89)90006-2.

Weber T, Wiseman N A, Kock A. 2019. Global ocean methane emissions dominated by shallow coastal waters. Nat Commun, 10: 4584, doi:10.1038/s41467-019-12541-7.

Weingartner T, Aagaard K, Woodgate R, et al. 2005. Circulation on the north central Chukchi Sea shelf. Deep Sea Res Part II Top Stud Oceanogr, 52(24-26): 3150-3174, doi:10.1016/j.dsr2.2005.10.015.

Weingartner T J, Cavalieri D J, Aagaard K, et al. 1998. Circulation, dense water formation, and outflow on the northeast Chukchi Shelf. J Geophys Res, 103(C4): 7647-7661, doi:10.1029/98jc00374.

Westbrook G K, Thatcher K E, Rohling E J, et al. 2009. Escape of methane gas from the seabed along the West Spitsbergen continental margin. Geophys Res Lett, 36(15): L15608, doi:10.1029/2009gl039191.

Whiticar M J, Faber E. 1986. Methane oxidation in sediment and water column environments—isotope evidence. Org Geochem, 10(4-6): 759-768, doi:10.1016/S0146-6380(86)80013-4.

Wiesenburg D A, Guinasso N L. 1979. Equilibrium solubilities of methane, carbon monoxide, and hydrogen in water and sea water. J Chem Eng Data, 24(4): 356-360, doi:10.1021/je60083a006.

Winkelmann D, Knies J. 2005. Recent distribution and accumulation of organic carbon on the continental margin west off Spitsbergen. Geochem Geophys Geosyst, 6(9): 117-134, doi:10.1029/2005 gc000916.

Woodgate R A, Aagaard K, Weingartner T J. 2005. A year in the physical oceanography of the Chukchi Sea: moored measurements from autumn 1990–1991. Deep Sea Res Part II Top Stud Oceanogr, 52(24-26): 3116-3149, doi:10.1016/j.dsr2.2005.10.016.